

Consequences of Increasing Packing Length on the Dynamics of Polymer Melts

Herwin Jerome Unidad,^{*,†} Mahmoud Abdel Goad,[‡] Ana Rita Bras,[‡] Michaela Zamponi,[†] Rudolf Faust,[§] Jürgen Allgaier,[‡] Wim Pyckhout-Hintzen,[‡] Andreas Wischnewski,[‡] Dieter Richter,[‡] and Lewis J. Fetters^{||}

[†]Jülich Centre for Neutron Science, Outstation at Heinz Maier-Leibnitz Zentrum, Forschungszentrum Jülich GmbH, Lichtenbergstraße 1, 85747 Garching, Germany

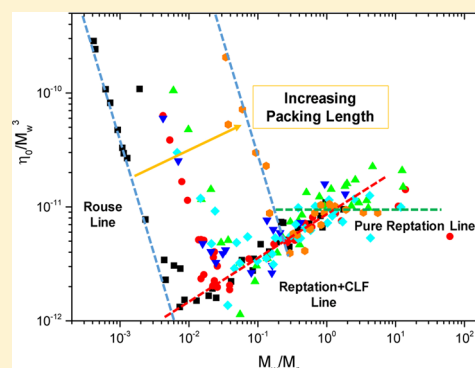
[‡]Jülich Centre for Neutron Science-1 and Institute of Complex Systems-1, Forschungszentrum Jülich GmbH, 52425 Jülich, Germany

[§]Chemistry Department, University of Massachusetts Lowell, Lowell, Massachusetts 01854, United States

^{||}Department of Chemical and Biomolecular Engineering, Cornell University, Ithaca, New York 14850, United States

S Supporting Information

ABSTRACT: We revisit the nonuniversal aspect of polymer dynamics by considering both new and existing data on the zero-shear viscosity and linear viscoelastic response of various polymers, each with a wide range of molecular weights. Analysis of the zero-shear viscosity data in terms of the packing length p , whose role in entanglements has been discussed previously by Fetters and co-workers, reveals a behavior that is irreconcilable with our current understanding based on the tube model. Specifically, we find that the transition regime between Rouse and pure reptation dynamics, currently understood as the regime where contour length fluctuations are active, systematically shrinks as the packing length of the polymer increases. Further, we find that the slope of the loss moduli in the high-frequency wing of the terminal peak of well-entangled systems also decreases from the common -0.25 to -0.125 with increasing p . This is contrary to the single expected value of -0.25 from tube models which include contour length fluctuations or -0.5 from pure reptation. These findings hint on possible missing ingredients in our current understanding of polymer dynamics.



INTRODUCTION

The tube model by de Gennes¹ as well as Doi and Edwards² is currently the most established framework for understanding polymer dynamics in the melt state. For the simplest possible case, which is that of monodisperse homopolymer melts with linear architecture, it is well-known that the dynamics of short chains is governed by Rouse behavior³ while that of long chains follows reptation¹ due to the presence of entanglements. Within this framework, which has been improved and developed by others,^{4–6} predictions for the scaling of the zero-shear viscosity η_0 with the molecular weight of the chain M_w are as follows:

1. for $M_w < M_c$: $\eta_0 \sim M_w$
2. for $M_c < M_w < M_r$: $\eta_0 \sim M_w^{3.4}$
3. for $M_w > M_r$: $\eta_0 \sim M_w^3$

where the transition values M_c and M_r are known as the *critical molecular weight* and *reptation molecular weight*, respectively. M_c marks the crossover from unentangled behavior (regime 1) to entangled behavior (regimes 2 and 3). The dynamics of unentangled chains are typically described in terms of the Rouse model³ while the dynamics of entangled chains are understood in terms of reptation¹ and the inherent limiting processes such as contour length fluctuations (CLF)⁴ and constraint release (CR).⁵ The effect of these limiting processes

vanishes for sufficiently long chains such that a second transition, marked by M_r is observed from entangled behavior due to reptation in combination with other processes (regime 2) to pure reptation (regime 3). In general, these scaling relations are well-reflected in experimental data from actual polymers, as shown for example in Figure 1.

While M_c marks the onset of entangled behavior in the melts, it is known that the actual length of an entanglement strand (i.e., of a subchain in between two entanglements) has another value M_e , called the *entanglement molecular weight*. In fact, it is well-known that $M_c/M_e \sim 2–4$ where the actual value of the ratio depends on the polymer.⁷ On the other hand, as mentioned earlier, the transition from 3.4 power scaling to the 3 power predicted by pure reptation which occurs around M_r has been rationalized by invoking the idea of contour length fluctuations, originally proposed by Doi⁴ and which consequently have been included in molecular theories of linear viscoelasticity.^{6,8} CLF is understood to be significant in relaxing stress near the chain ends in addition to stress relaxation by reptation, and its effect is quite significant for modest chain

Received: February 16, 2015

Revised: August 20, 2015

Published: August 28, 2015

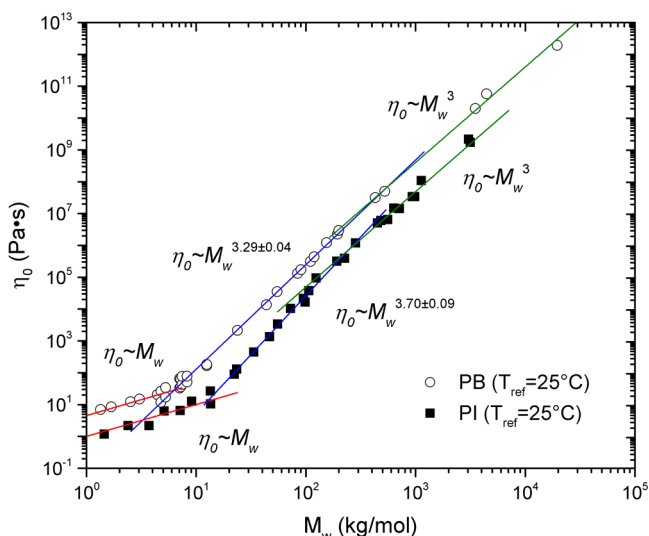


Figure 1. Experimental data for the zero-shear viscosity as a function of molecular weight of polybutadiene (PB) and polyisoprene (PI) melts. Data are obtained from various sources^{9,11,12} and show the three scaling regimes. Lines show the different power law fits for each regime.

lengths though somewhat less significant for suitably large chain lengths. This means that beyond a certain critical length (M_r) the effect gives way to pure reptation. Note that in the literature this crossover to pure reptation has been observed only for a few cases.^{9–11}

As for entangled dynamics itself, the tube model by Doi and Edwards predicts that the large-scale behavior of chains in a homopolymer melt is universal and emerges simply from a fundamental length scale called the tube diameter a , also to be interpreted as the end-to-end distance of an entanglement strand or the step length of the tube. The entanglement molecular weight M_e then corresponds to the molecular weight of a polymer strand between two entanglements and spanning the distance a . From the perspective of the tube model, M_e serves as a polymer-specific input that allows one to determine the number of entanglements $Z = M_w/M_e$ which is the sole determinant of dynamical behavior; i.e., different polymers with the same Z have dynamics that can be rescaled to coincide purely by their difference in the basic length scale (a or M_e) and time scale (τ_e , the relaxation time of an entanglement strand). In the literature, various models have been proposed to predict how M_e emerges from chain properties such as local stiffness and conformation.^{13–18} Experimentally, M_e is typically determined from the plateau modulus G_0 , an expected signature of entanglement-dominated behavior during stress relaxation.

In a series of landmark papers,^{19–21} Fetters and co-workers presented a systematic investigation of the values of M_e , M_v , and M_r across a wide variety of polymers whose data are available in the literature. First, they were able to show a systematic correlation between equilibrium chain dimensions $\langle R^2 \rangle_0$ and entanglement behavior (G_0 or M_e) through the parameter p called the packing length which is defined as

$$p = \frac{M_w}{\rho N_A \langle R^2 \rangle_0} \quad (1)$$

where ρ is the polymer density and N_A is Avogadro's number. M_e and G_0 are then related to p as follows

$$M_e = n_t^2 N_A \rho p^3 \quad (2)$$

$$G_0 = \frac{\rho RT}{M_e} = \frac{RT}{n_t^2 N_A p^3} \quad (3)$$

where T is the temperature, R is the ideal gas constant, and n_t is basically a weakly temperature-dependent dimensionless number corresponding to the number of entanglement strands present per cube of the tube diameter with a value of approximately 21 as determined from experimental data by Fetters et al.^{19,20} and consistent with predictions from chain packing arguments by Lin¹⁶ and Kavassalis and Noolandi.^{13–15} The above equations then establish a clear relationship between microscopic, chemistry-dependent details and the rheology or global chain dynamics of polymer melts.

Second, they show a systematic variation of the two transition molecular weights as a function of p . Phenomenologically, they find from examining data on different polymers that M_c and M_r each scale differently with p as follows:

$$M_c = M_c \left[\frac{p^*}{p} \right]^{-0.65} = n_t^2 N_A \rho (p^*)^{0.65} p^{-2.35} \quad (4)$$

$$M_r = M_r \left[\frac{p^*}{p} \right]^{3.9} = n_t^2 N_A \rho (p^*)^{3.9} p^{-0.9} \quad (5)$$

where p^* has a value of about 9.2 Å. Note that eq 5 was derived in the original paper²⁰ based on only two data points (i.e., two values of p) and should be used with caution. Later, we will present an updated version of eqs 4 and 5 in light of new data. Nonetheless, the implications of these equations are astounding in our opinion since they imply a packing-length dependence of the crossover molecular weights and, more surprisingly, a convergence and intersection of M_v , M_e , and M_r for $p = p^*$! This would have significant effects on the dynamics since it anticipates a p -dependent shrinking of the regime where contour length fluctuations have a dominant contribution. As one increases p , a point might be reached where the contribution of contour length fluctuations could vanish! This fact is currently unaccounted for within the standard tube model framework and has not been discussed extensively in the polymer dynamics community. To the best of our knowledge, the only acknowledgment of the implications of these findings is that of McLeish,²² who remarked on the connection between the existence of M_c and M_r and the significance of CLF for intermediate chain lengths (i.e., CLF being responsible for the 3.4-power law scaling of η_0).

In this work, following the original spirit of the packing length papers,^{19–21} we present a systematic examination of a combination of existing literature data as well as of new data from our experiments for various polymer melts on the zero-shear viscosity scaling as a function of molecular weight and on the linear viscoelastic response as a function of frequency. This data set includes measurements for the polymer polyvinylcyclohexane (PVCH) which has a particularly large value of p and of polyisobutylene (PIB) in the low-to-intermediate molecular weight range, both of which have not been examined yet in the literature. This enabled us to expand the earlier compilation of Fetters et al.²⁰ since we now consider six well-characterized and monodisperse polymers with different packing lengths. This strengthens our conclusions regarding the packing length dependence of the chain dynamics. Different from this earlier work which focused solely on the plateau modulus and various

Table 1. Data Sources in the Literature for the Viscosity Measurements and Various Parameters for the Different Polymer Melts

polymer and data sources	p [Å]	T_{ref} [°C]	M_c [kg/mol]	M_e [kg/mol]	M_r [kg/mol]
polyethylene (PE) ^{23,24}	1.69	175	1.2	4.5 ± 1.1	621.8 ± 3.0
polybutadiene (PB) ⁹	2.12	25	2.2	6.3 ± 1.1	532.1 ± 3.2
polyisoprene (PI) ^{11,12}	3.10	25	6.2	12.7 ± 1.1	244.8 ± 2.2
polyisobutylene (PIB) ¹⁰	3.17	25	6.7	11.1 ± 1.4	436.5 ± 11.8
polystyrene (PS) ^{25–28}	3.95	160	17	29 ± 1	624 ± 4
polyvinylcyclohexane (PVCH) ²⁹	5.59	180	50	90 ± 2	379 ± 15

transition molecular weights,^{19–21} our work examines zero-shear viscosity data (η_0) for a broad range of molecular weights—hereby giving an alternative though complementary approach and a more complete picture for arriving at the same conclusions. In addition, we examine the linear viscoelastic response, particularly the loss modulus $G''(\omega)$, for four different polymers with rather similar number of entanglements but with different packing lengths. This allows us to scrutinize the universality of features built into quantitative formulations of the tube model with CLF.⁶ Both data sets suggest missing ingredients in our current theoretical description of viscoelasticity and polymer dynamics.

EXPERIMENTAL DETAILS

In this study, we considered a combination of zero-shear viscosity data from both literature and measurements done in our laboratory on six different polymers: polyethylene (PE), polybutadiene (PB), polyisoprene (PI), polystyrene (PS), polyisobutylene (PIB), and polyvinylcyclohexane (PVCH). The latter is also known as polycyclohexylethylene (PCHE) in the literature. Data for PVCH, which also has the largest value for p , its parent PS, and the low molecular weight PIB melts, stem mainly from our own measurements. A complete list of all the sources for compiling the data set for all these polymers is presented in Table 1. Note that since we use multiple sources with different associated experimental uncertainties that the different quantities from our analysis may show deviations from previously known values.

Measurements on all the polymers considered here were done on samples prepared by anionic polymerization except for the PIB data. Those from Fetters et al.¹⁰ were obtained from commercial sources ($M_w/M_n \leq 1.4$), and the present extension of lower molecular weight samples was prepared via cationic polymerization ($M_w/M_n \leq 1.2$). The PE, PEP, and PVCH samples were prepared by hydrogenation of the parent PB, PI, and PS. Those materials, in turn, retained the near monodisperse nature of the parent polydienes and polystyrene which were synthesized by lithium head groups in hydrocarbon solvents. Thus, the polyolefinic samples had $M_w/M_n < 1.1$ expected for samples from living anionic polymerizations. Hence, for all polymers other than the high molecular weight PIB, polydispersity is not a significant concern. In the case of PVCH only, the highest molecular weights suffered slightly from the hydrogenation procedure ($M_w/M_n < 1.2$). Further details on the characterization of the polymers used for our own measurements can be found in the Supporting Information.

In addition, we measured the loss moduli of four different polymers: polyethylene propylene (PEP), PI, PS, and PVCH with comparable number of entanglements ($Z = M_w/M_e = 25 \pm 4$). Other parameters pertaining to these samples are reported in Table 2.

Linear rheology measurements of our own samples were performed on an ARES rheometer (Rheometric Scientific Instruments) equipped with a 2k-FRNT transducer under a nitrogen blanket to prevent sample degradation. Data for each polymer are shifted to a common reference temperature T_{ref} while the lower molecular weight samples were measured at a shifted T to comply with the isofrictional condition (i.e., same distance from the glass transition temperature T_g estimated from the known chain length-dependence of T_g ⁷). These corrections were done within each polymer type.

Table 2. Material Characteristics of the Polymers for Loss Moduli Measurements

polymer	p [Å]	T_{ref} [°C]	M_w [kg/mol]	M_e [kg/mol]	Z
poly(ethylene- <i>alt</i> -propylene) (PEP)	2.10	25	67.3	2.25	30
polyisoprene (PI)	3.10	25	128	6.2	21
polystyrene (PS)	3.95	160	417	17	25
polyvinylcyclohexane (PVCH)	5.59	180	1230	50	25

The values of the entanglement molecular weight (M_e) reported in Tables 1 and 2 are calculated using eq 3 using our measured values for the plateau modulus (G_0) except for PE and PIB, which were then taken from the compilation of Fetters et al.^{20,30} The values of the critical molecular weight (M_c) and the reptative molecular weight (M_r) are obtained from our compiled data sets by fitting the various regions of the η_0 vs M data with power laws corresponding to the Rouse, reptation-CLF, and pure reptation regimes and calculating their intersections. The reported errors are obtained by propagating the standard error associated for each fitting. These fittings are detailed in the Supporting Information. In most cases, the values we obtained for these molecular weights compare reasonably with previously known values in the compilation of Fetters et al.^{20,30}

RESULTS AND DISCUSSION

Zero-Shear Viscosity Data. The zero-shear viscosity data compiled for various polymers with different molecular weights are shown in log–log format in Figure 2. The x -axis is the molecular weight normalized by the critical molecular weight M_c , whose values are reported in Table 2, while the y -axis is the zero-shear viscosity η_0 normalized by the predicted scaling of M_w^3 from reptation theory¹ and shifted vertically with an arbitrary factor to delineate each curve. The normalization in the x -axis allows comparison of the unentangled–entangled transition for each polymer melt by aligning all the reduced viscosity minima at the same point. At the same time, the normalization of the y -axis, as previously done by others,^{6,11,12} highlights the three regimes of dynamical behavior for polymer melts as one goes from low to high molecular weight: the Rouse regime ($\eta_0 \sim M_w$), which manifests as a negative slope of -2 in the plot; the entanglement-dominated regime ($\eta_0 \sim M_w^{3.4}$) where mechanisms such as reptation, CLF, and CR are held to be active,^{4,6} which shows as a slight positive slope of 0.4; and the pure reptation regime ($\eta_0 \sim M_w^3$), which is the leveling off to 0 slope. Note that the differences in the levels of the η_0/M_w^3 curves may arise from the different reference temperatures (Table 1) and, correspondingly, the different monomer friction values for each polymer. However, in this log–log representation, shifting the viscosity curves to other reference temperatures, for example such that curves corresponding to each polymer are at the same distance from T_g (isofrictional condition), would result only in a vertical shifting of the curve with no changes in the curve shape.

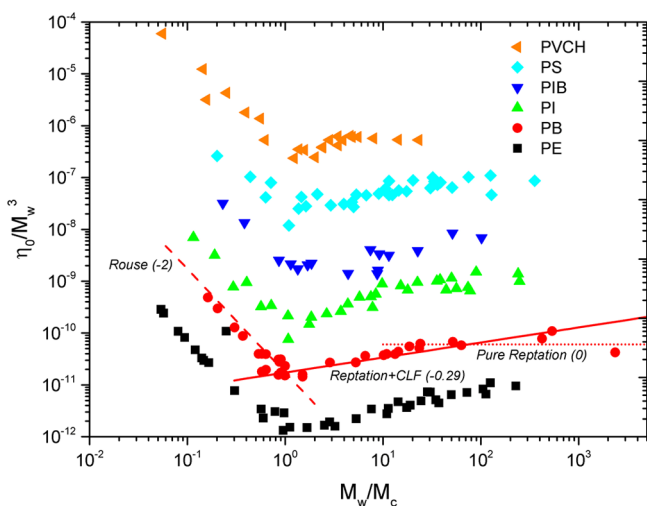


Figure 2. Reduced absolute zero-shear viscosity data as a function of the molecular weight normalized with respect to M_c and with an arbitrary vertical shift for each polymer data set at a polymer-specific reference temperature. Examples of the power law fits are shown for the PB data set.

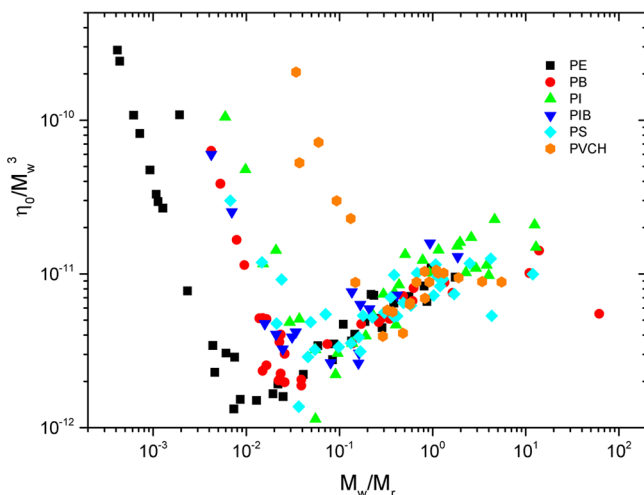


Figure 3. Normalized zero-shear viscosity data as a function of the molecular weight normalized with M_r for various polymers. Curves are shifted vertically to make the pure reptation regime (0 slope) coincide.

It is apparent in Figure 2 that there is variation in the “triangular area” of the curve (formed by the -2 and 0.4 slope lines) depending on the polymer type with PE having the largest “triangle” and PVCH having the smallest. Indeed, since the vertices of the triangles (corresponding to the M_c crossover point) are aligned vertically, one can see that it is the 0.4 slope line that varies for each type of polymer.

The data can be better understood, with respect to the different dynamic regimes and crossover points, by normalizing the molecular weight with the reptation molecular weight (M_r) as shown in Figure 3. The value for M_r for each polymer is obtained from the crossover of the 3.4 slope and 3 slope lines in the η_0 vs M_w as discussed previously. In Figure 3, the viscosity curves are shifted vertically for better comparison across polymers by making the 0.4 slope and 0 slope lines coincide about their intersection while normalizing the x -axis with M_r .

Figure 3 shows the variation of the extent of the 3.4 power law regime for the various polymers. The normalization and

shifting with M_r also make the packing length dependence of the trend more apparent since in Figure 3, the pure reptation lines all coincide while the Rouse lines follow a trend of increasing p as one goes from left to right. Here, the shrinking of the 0.4 slope line as one goes to larger p becomes most apparent. Despite the scatter in the data, which come from various sources, the trends are clear.

It should be clarified that while the packing length dependence of M_c , M_c , and M_r has already been presented previously by Fetters et al.,²⁰ its possible implications in the dynamics has not received attention in the polymer physics community since most investigated polymers are clustered in the packing length range of $p = 1.8$ – 4 , which would correspond to $M_c/M_e = 1.7$ – 3 . The fact that $M_c \sim (2$ – $3)M_e$ is actually well-known and often mentioned in textbooks though no clear physical reason for the variation of this factor is given. Further, the transition to pure reptation in the viscosity (or in the terminal relaxation time³¹) was observed only for a few polymers,^{9–11,31} all within the same packing length range. However, when one looks at polymers with $p > 5$, as in our case with PVCH ($p = 5.59$), one can see that the 3.4 power law regime is actually quite short, and one reaches the pure reptation power law regime with $Z < 10$, since $M_r/M_e = 7.6$. This fact is remarkable in our opinion since standard tube theories such as that of Likhtman and McLeish⁶ predict the transition to the pure reptation regime around $Z \sim 1000$!

To illustrate this further, we show the obtained $Z_c = M_c/M_e$ and $Z_r = M_r/M_e$ for all the polymers considered in this work in Figure 4. In Figure 4, the error-weighted power law fits we

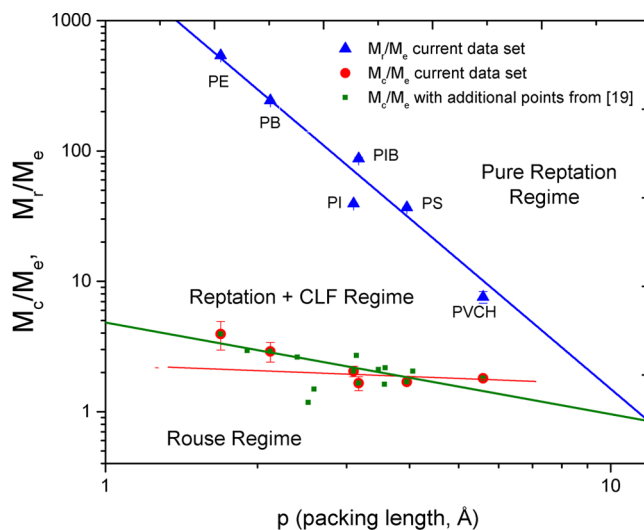


Figure 4. Values of Z corresponding to the transition to Rouse to reptation + CLF to pure reptation regimes as a function of p .

obtained for both M_c and M_r as a function of p for the six polymers we considered are shown as the thin red line and the thick blue line, respectively. However, since more M_c values for other polymers are available,²⁰ we augmented our data set for M_c with these values. The resulting fit for this extended data set is shown by the thick green line. The equations corresponding to the thick green and blue lines are

$$\frac{M_c}{M_e} = 0.68p^{-0.70} = \left[\frac{p^*}{p} \right]^{0.70} \quad (6)$$

$$\frac{M_r}{M_c} = 3.46p^{-3.29} = \left[\frac{p^*}{p} \right]^{3.29} \quad (7)$$

where the exponents 0.70 and 3.29 are similar to those obtained by Fetters et al. in their earlier compilation of data²⁰ while $p^* = 11.8 \pm 1.4 \text{ \AA}$, a value higher than the previous estimate.

Figure 4 also highlights how one traverses the different dynamical regimes as one increases in molecular weight (as a multiple of M_c) for each packing length value. For polymers with $p \sim 1.8\text{--}4$, which is where most polymer melts investigated using rheology lie, one goes from Rouse dynamics (for $Z < Z_c$) to the entangled dynamics with both reptation and CLF (for $Z_c < Z < Z_r$) to pure reptation dynamics (for $Z > Z_r$). In the plot, the p -dependence of these transition points are highlighted, and it is apparent that one can enter the pure reptation regime with much lower Z for polymers with sufficiently large p . Further, since we confirm the convergence of both M_c and M_r at a value of $p \approx 12$, we note that the transition along the intersection point (p^*) and beyond would be interesting since one goes directly from Rouse to pure reptation dynamics! Currently, no viscosity data are available for polymers with such large packing lengths although they have been the subject of previous work.^{30,32,33}

At present, it is not fully clear to us why the direct transition from Rouse to pure reptation dynamics could occur for such polymers or, similarly, why the relaxation process would bypass the regime where contour length fluctuations are dominant. Indeed, while CLF is an inherently faster process than reptation that allows fast stress relaxation around the chain ends, one can expect this process to give way to the much slower process of reptation only if one would consider CLF as an activated process. However, this point needs further investigation.

Note also that the interpretation of the observed 3.4 power law as being due to single-chain effects, mostly the interplay of reptation and CLF as first proposed by Doi,⁴ was challenged recently by “probe rheology” experiments of moderately entangled chains in a matrix of very long chains.^{34,35} In these experiments, by making an environment of entanglements that are permanent in the time scale of the shorter chains, they are able to switch off the many-chain constraint release (CR) contribution to the stress relaxation while keeping the single-chain contributions of reptation and CLF the same. They observed that the longest relaxation time τ_d for the case of the blend scaled as $\tau_d \sim M_w^{3.1}$ compared to the case of the pure melt where it scaled as $\tau_d \sim M_w^{3.4}$. Given that only the CR contribution was altered by making the blend, they hereby argue that the observed 3.4 power law for melts cannot be wholly attributed to CLF and must, in part, also emerge from CR. This is also consistent with results from neutron spin-echo experiments which reveal a molecular weight dependence of the balance between CLF and CR.^{36,37} A quantitative comparison could be made, however, with the dynamic modulus of unattached chains in a permanent network.³⁸ Here, a narrowing of the $G''(\omega)$ is found as well as the expected $\omega^{-1/2}$ slope for pure reptation. The network hereby switched off both CR and CLF and indirectly shows that hairpin excursions are connected with CLF.

The interpretation of this probe rheology data was, however, challenged by slip-link simulations by Schieber et al.³⁹ which show that actual dynamics of the constraints could in fact give rise to the extra stress relaxation measured. Their findings reaffirm the explanation of Doi⁴ for the monodisperse case.

Nevertheless, whether one follows the classical single-chain interpretation^{4,6} or this many-chain interpretation,³⁵ it is clear from the results we present here that the current theoretical framework cannot universally capture all the available data and some other ingredients are missing in the current framework. Indeed, we affirm that the p -dependence of the dynamics cannot be ignored in light of the results we present here and that a universal description of polymer dynamics is still possible, but it must necessarily include these p -dependent effects. In the following section, we make the case that these p -dependent effects might be strongly related to the description of contour length fluctuations.

Loss Moduli. To further understand the role of the packing-length p in entangled dynamics, we examined the full linear viscoelastic spectra for a series of polymers with different packing lengths ($p = 2.0\text{--}5.5$) and with similar number of entanglements ($Z = M_w/M_c = 25 \pm 4$). Since the polymers are well-entangled (as opposed to only weakly entangled, e.g., $Z \sim 5$), the system is expected to be well within the known regime of validity of tube models for linear viscoelasticity. This degree of entanglement is expected to lead to a well-pronounced single -0.25 slope behavior in the high-frequency wing of the terminal peak in the loss modulus, with no signature of the -0.5 slope attributed to pure reptation. Recent formulations of the tube model⁶ as well as the emerging class of slip-link models^{40,41} would predict that these systems would behave similarly or, more specifically, that their linear viscoelastic spectra could be superimposed by scaling the basic units for the stress level (plateau modulus, G_0) and the time scale (characteristic time of the entanglement strand, τ_e). Here, we show that this is not necessarily the case, at least as far as the loss moduli G'' is concerned.

Figure 5 shows the obtained loss moduli for the four polymers considered (PEP, PI, PS, PVCH) whose characteristics are reported in Table 2. The moduli were shifted to a reference temperature by time–temperature superposition,⁷ and the differences in the position of the terminal relaxation peak in the x -axis and y -axis correspond to the differences in the basic units of time (τ_e) and stress/moduli (G_0) at this temperature for the four systems.

For better appraisal, we arbitrarily shift the spectra in both the frequency and modulus axes to make the minima coincide—hereby normalizing the data with respect to a reference polymers, in this case PEP (the lowest p). The result of this shifting is shown in Figure 6. This normalization allows us to isolate the effect of the glassy modes that dominate the relaxation beyond the minimum of the loss modulus. One can see while the terminal peaks do not fully coincide (due to the actual differences in Z), the decrease in the high frequency slope of the terminal region with increasing p can be clearly appraised. Since we normalized the data with respect to the minima, we isolate the role of the glassy mode relaxation in this intermediate frequency range since all the polymers effectively will have similar glassy mode contributions (isofrictional condition). This is shown by the parallel and almost coincident high-frequency behavior after the minima. This means that the variation in the slope we observe at the intermediate frequency range must be related to more global chain dynamics.

To describe this variation quantitatively, we fit the data with the phenomenological relaxation spectrum suggested by Baumgärtel, Schausberger, and Winter (BSW).⁴² Further details on the functional form for this fit can be found in their original paper. We note that the data itself already reveals the qualitative

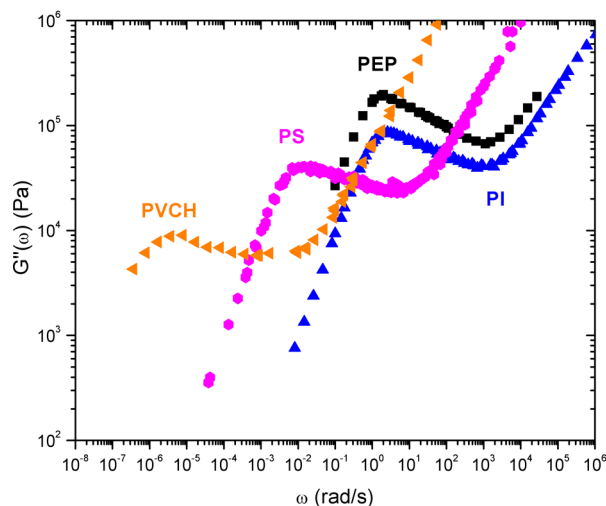


Figure 5. Loss moduli for the polymer melts with different packing lengths $p = 2.0$ – 5.5 but with comparable number of entanglements $Z = M_w/M_e = 25 \pm 4$ each shifted to the reference temperature of Table 1.

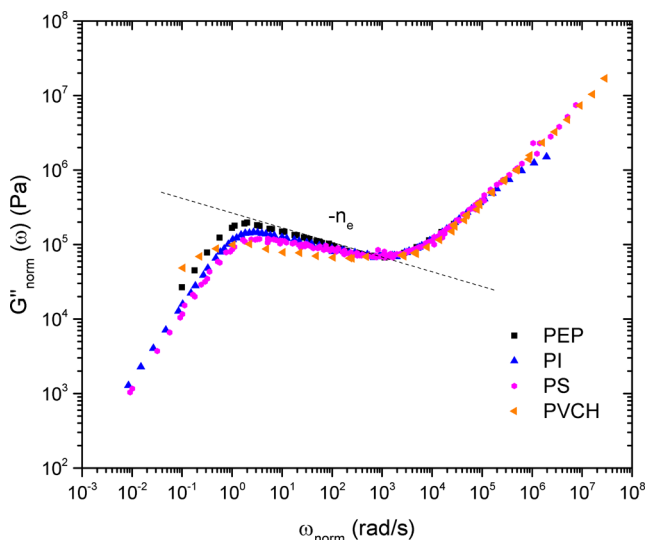


Figure 6. Horizontally and vertically shifted loss moduli from Figure 5 corresponding to an effective normalization along the glassy mode contributions that dominate after the minimum. Dashed line shows the slope $-n_e$ plotted in Figure 7.

behavior, and the BSW approach is used only to capture this dependence more quantitatively into a more physical parameter, n_e . The parameter n_e (alternatively, n_1 in the original BSW paper⁴²) gives the negative of the high-frequency slope of the terminal relaxation peak in this CLF-dominated molecular weight range after accounting for the crossover to the glassy modes. It should be made clear that the n_e exponent is the real slope, and not the effective one, since the BSW approach already accounts for the glassy modes in the range of frequencies where n_e is determined. Results from fitting n_e for the different polymers are shown in Figure 7. We clarify that these reported values for n_e are the fitted values for the samples described in Table 2, i.e., for samples with comparable degrees of entanglement $Z \approx 25$. This means that all polymers considered are well-entangled with a wide separation between the minimum of the loss modulus and the terminal relaxation peak, i.e., a frequency range of about 3 decades where n_e can be

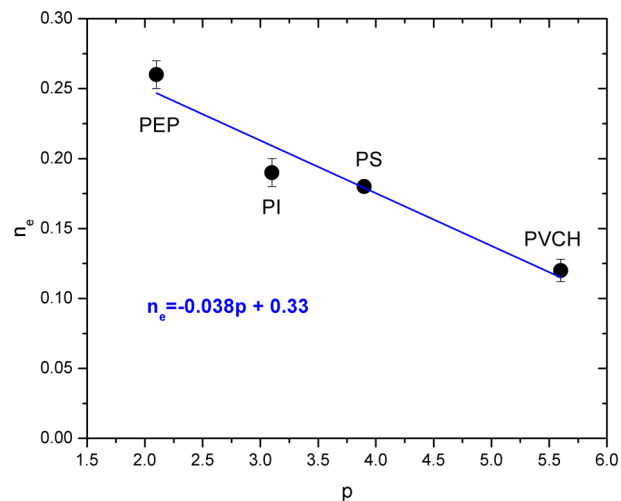


Figure 7. Fitted values for the high-frequency slope of the terminal relaxation peak from Figure 6 obtained using the BSW spectrum.⁴²

fitted. This also means that all polymers have similar levels of contamination by glassy modes in the same frequency range. We isolate this visually via the normalization about the minimum, as in Figure 6, and quantitatively using the BSW spectrum.

Tube models which include contour length fluctuations, for example that by Likhtman and McLeish,⁶ predict n_e to be -0.25 . On the contrary, we find that the slope actually varies with p from about -0.25 for the lowest p -polymer considered (PEP) up to about -0.125 for the highest p -polymer (PVCH) which, as in the previous section, also has the narrowest regime for the $\eta_0 \sim M_w^{3.4}$ scaling. This decrease of slope which we observe could in fact indicate a p -dependence in the effectiveness of contour length fluctuations as a limiting process to reptation or of additional modes or processes that are not treated yet by present tube or slip-link models.

Curiously, if we expect CLF to be less effective in relaxing stress and to give way to pure reptation for large- p polymers, then our present understanding of polymer dynamics suggest that the loss modulus should be narrower and more symmetric following $\omega^{-1/2}$ or n_e of -0.5 as CLF is no longer active in broadening the terminal relaxation peak by introducing faster processes. However, we observe the opposite trend in Figure 6 and see an effective broadening of the terminal relaxation. Alternatively, one can interpret this as a flattening of the G'' as it approaches and becomes parallel to G' , which in this frequency range shows the entanglement plateau. This could happen in the limit of large packing length values, i.e., $p \approx p^*$. This could also indicate that polymers at this p range could have both Rouse-like features such as the parallel and coincident G' and G'' as well as entangled features such as the plateau modulus. Such features are not anticipated by our current theories for chain dynamics in the melt.

It is also important to point out that others in the literature have already identified shortcomings of the current theory for contour length fluctuations.^{43–45} Particularly problematic is the description of mildly entangled polymers (i.e., only slightly above the critical molecular weight M_c). However, all these efforts to amend the current description^{43–45} still operate in the universality framework where only one polymer-specific length-scale is considered (a or, equivalently, M_e and G_0 , the last two of which are known to have model-dependent relation-

ships^{2,46,47}). In the data we presented in this section, which concerns well-entangled systems, we find that the tube/slip-link description^{6,40} where the only effective parameter is Z (after normalizing with G_0 and τ_e) still cannot capture the viscoelastic spectra across polymers with varying p or, at least, not simply through the current normalization. We propose here based on the collection of data for η_0 and $G''(\omega)$ we presented that a second, more microscopic length scale, namely the packing length p , must enter in the current modeling framework if we seek to fit available data quantitatively. As p depends on a combination of local stiffness and bulkiness of monomer units, it is possible that the current coarse-grained description where all local details are somewhat subsumed in the basic units for stress and time are already deficient in capturing the rich dynamics of entangled systems.

CONCLUSIONS

In this work, we revisited the nonuniversal aspect of polymer dynamics by confronting viscosity and rheology data from various polymers, combining both measurements in the literature and our own results, and analyzing these in terms of the packing length concept.^{19,20} In considering the zero-shear viscosity data for six different polymer melts, we found a packing-length-dependent reduction of the intermediate region in the zero-shear viscosity scaling, i.e., the transition regime between Rouse and pure reptation dynamics typically attributed to the competition between reptation and contour length fluctuations. Further, plotting the crossover molecular weights (M_c , M_r) as a function of the packing length (p), we reconfirm the previous finding of Fetters and co-workers²⁰ that both also exhibit power law dependence with p . These power laws were also found to intersect at a critical value for the packing length (p^*), here estimated to be about 11.8 Å.

Further, by considering the linear viscoelastic response of melts with similar levels of entanglement but with different values of the packing length, we find packing-length-dependent features of the loss modulus $G''(\omega)$. Specifically, we find that while the high frequency part of the relaxation corresponding to the glassy modes can be made to coincide, the slope in the intermediate frequency range (i.e., in the high frequency side of the terminal peak) exhibits a variation with increasing packing length. In the molecular weight range of about 25 entanglement lengths, we find a slope of about -0.25 for the polymer with the lowest packing length and a slope of -0.125 for the polymer with the highest packing length.

The above findings seem to indicate an understated role of the packing length as an additional length scale in entangled dynamics, particularly in the current description of CLF. However, we do not exclude the possible contribution of constraint release (and its interplay with CLF) and other limiting processes, especially since the two give related signatures in microscopic dynamics^{36,37} as probed, for example, by neutron spin-echo spectroscopy. In any case, our aim in presenting our findings is to stimulate further discussion on the subject which could lead to improvements in the current theoretical picture.

In addition, further investigations on melts with even larger packing lengths should prove to be interesting given our anticipation that the crossover molecular weights would intersect at larger values of p . At present, no viscosity data from polymers with $p > p^*$ seem to be available although some melts with p values larger than the range we presented here have been the subject of recent work.^{30,32,33} We hope that such

data would be available in the future to improve our current understanding.

ASSOCIATED CONTENT

Supporting Information

The Supporting Information is available free of charge on the ACS Publications website at DOI: 10.1021/acs.macromol.5b00341.

Further details on the preparation and characterization of polymer samples whose linear viscoelastic properties we measured, in particular, including PEP, PIB, PS, and PVCH of various molecular weights; further details on the fitting of zero-shear viscosity data with power laws to obtain values for M_c and M_r , (PDF)

AUTHOR INFORMATION

Corresponding Author

*E-mail: h.unidad@fz-juelich.de (H.J.U.).

Notes

The authors declare no competing financial interest.

REFERENCES

- (1) de Gennes, P. *J. Chem. Phys.* **1971**, *55*, 572–579.
- (2) Doi, M.; Edwards, S. *The Theory of Polymer Dynamics*; Oxford University Press: New York, 1986.
- (3) Rouse, P. *J. Chem. Phys.* **1953**, *21*, 1272.
- (4) Doi, M. *J. Polym. Sci., Polym. Phys. Ed.* **1983**, *21*, 667–684.
- (5) Graessley, W. *Adv. Polym. Sci.* **1982**, *47*, 69–117.
- (6) Likhtman, A.; McLeish, T. *Macromolecules* **2002**, *35*, 6332–6343.
- (7) Ferry, J. *Viscoelastic Properties of Polymers*; John Wiley & Sons: New York, 1980.
- (8) van Ruymbeke, E.; Keunings, R.; Bailly, C. *J. Non-Newtonian Fluid Mech.* **2005**, *128*, 7–22.
- (9) Colby, R.; Fetters, L.; Graessley, W. *Macromolecules* **1987**, *20*, 2226–2237.
- (10) Fetters, L.; Graessley, W.; Kiss, A. *Macromolecules* **1991**, *24*, 3136–3141.
- (11) Abdel-Goad, M.; Pyckhout-Hintzen, W.; Kahle, S.; Allgaier, J.; Richter, D.; Fetters, L. *Macromolecules* **2004**, *37*, 8135–8144.
- (12) Auhl, D.; Ramirez, J.; Likhtman, A.; Chambon, P.; Fernyhough, C. *J. Rheol.* **2008**, *52*, 801–835.
- (13) Kavassalis, T.; Noolandi, J. *Phys. Rev. Lett.* **1987**, *59*, 2674–2677.
- (14) Kavassalis, T.; Noolandi, J. *Macromolecules* **1988**, *21*, 2869–2879.
- (15) Kavassalis, T.; Noolandi, J. *Macromolecules* **1989**, *22*, 2709–2720.
- (16) Lin, Y. *Macromolecules* **1987**, *20*, 3080–3083.
- (17) Heymans, N. *Macromolecules* **2000**, *33*, 4226–4234.
- (18) Wang, S. *Macromolecules* **2007**, *40*, 8684–8694.
- (19) Fetters, L.; Lohse, D.; Richter, D.; Witten, T.; Zirkel, A. *Macromolecules* **1994**, *27*, 4639–4647.
- (20) Fetters, L.; Lohse, D.; Milner, S.; Graessley, W. *Macromolecules* **1999**, *32*, 6847–6851.
- (21) Fetters, L.; Lohse, D.; Graessley, W. *J. Polym. Sci., Part B: Polym. Phys.* **1999**, *37*, 1023–1033.
- (22) McLeish, T. *Rheol. Rev.* **2003**, 197–233.
- (23) Pearson, D.; ver Strate, G.; von Meerwall, E.; Schilling, F. *Macromolecules* **1987**, *20*, 1133–1141.
- (24) Pearson, D.; Fetters, L.; Graessley, W.; ver Strate, G.; von Meerwall, E. *Macromolecules* **1994**, *27*, 711–719.
- (25) Allen, V.; Fox, T. *J. Chem. Phys.* **1964**, *41*, 337–343.
- (26) Fox, T.; Allen, V. *J. Chem. Phys.* **1964**, *41*, 344–352.
- (27) Schausberger, A.; Schindlauer, G.; Janeschitz-Kriegl, H. *Rheol. Acta* **1985**, *24*, 220–227.
- (28) Schindlauer, G.; Schausberger, A.; Janeschitz-Kriegl, H. *Rheol. Acta* **1985**, *24*, 228–231.

- (29) Zhao, J.; Hahn, S.; Hucul, D.; Meunier, D. *Macromolecules* **2001**, *34*, 1737–1741.
- (30) Fetters, L.; Lohse, D.; Garcia-Franco, C.; Brant, P.; Richter, D. *Macromolecules* **2002**, *35*, 10096–10101.
- (31) Abou Elfadl, A.; Kahlau, R.; Herrmann, A.; Novikov, V.; Rossler, E. *Macromolecules* **2010**, *43*, 3340–3351.
- (32) Gerstl, C.; Schneider, G.; Pyckhout-Hintzen, W.; Allgaier, J.; Willbold, S.; Hofmann, D.; Disko, U.; Frielinghaus, H.; Richter, D. *Macromolecules* **2011**, *44*, 6077–6084.
- (33) Andreozzi, L.; Galli, G.; Giordano, M.; Zulli, F. *Macromolecules* **2013**, *46*, 5003–5017.
- (34) Liu, C.; Halasa, A.; Keunings, R.; Bailly, C. *Macromolecules* **2006**, *39*, 7415–7424.
- (35) Liu, C.; Keunings, R.; Bailly, C. *Phys. Rev. Lett.* **2006**, *97*, 246001.
- (36) Zamponi, M.; Monkenbusch, M.; Willner, L.; Wischniewski, A.; Farago, B.; Richter, D. *Europhys. Lett.* **2005**, *72*, 1039–1044.
- (37) Zamponi, M.; Wischniewski, A.; Monkenbusch, M.; Willner, L.; Richter, D.; Likhtman, A.; Kali, G.; Farago, B. *Phys. Rev. Lett.* **2006**, *96*, 238302.
- (38) Ndoni, S.; Vorup, A.; Kramer, O. *Macromolecules* **1998**, *31*, 3353–3360.
- (39) Khaliullin, R.; Schieber, J. *Macromolecules* **2010**, *43*, 6202–6212.
- (40) Masubuchi, Y.; Ianniruberto, G.; Greco, F.; Marrucci, G. *J. Non-Newtonian Fluid Mech.* **2008**, *149*, 87–92.
- (41) Khaliullin, R.; Schieber, J. *Macromolecules* **2009**, *42*, 7504–7517.
- (42) Baumgärtel, M.; Schausberger, A.; Winter, H. *Rheol. Acta* **1990**, *29*, 400–408.
- (43) Hou, J.; Svaneborg, C.; Everaers, R.; Grest, G. *Phys. Rev. Lett.* **2010**, *105*, 068301.
- (44) van Ruymbeke, E.; Vlassopoulos, D.; Kapnistos, M.; Liu, C.; Bailly, C. *Macromolecules* **2010**, *43*, 525–531.
- (45) Qin, J.; Milner, S.; Stephanou, P.; Mavrantzas, V. *J. Rheol.* **2012**, *56*, 707.
- (46) Larson, R.; Sridhar, T.; Leal, L.; McKinley, G.; Likhtman, A.; McLeish, T. *J. Rheol.* **2003**, *47*, 809–818.
- (47) Masubuchi, Y.; Ianniruberto, G.; Greco, F.; Marrucci, G. *J. Chem. Phys.* **2003**, *119*, 6925–6930.